February 26, 2004

Dr. Harin Ullal
Mail Stop 3212
National Renewable Energy Laboratory
1617 Cole Blvd
Golden, CO 80401-3393

Re: Phase II, Third Quarterly Report #ZDJ-2-30630-14

Dear Harin,

This letter comprises the quarterly technical status report for Thin Film Partnership subcontract # ZDJ-2-30630-14. The reported work was performed during the third quarter of year 2 for this contract, from 11/15/03 to 2/15/03. This report describes activities performed by GSE, as well as those performed by lower-tier subcontractor ITN Energy Systems, Inc.

1. INTRODUCTION

Two-stage and three-stage CIGS coevaporation – followed by chemical bath CdS and RF-sputtered resistive and conductive ZnO – have come to be viewed as laboratory standards for the deposition of CIGS photovoltaic devices. However, a number of conditions are encountered during continuous manufacturing that prevent an exact replication of the laboratory processes. Such differences include both those imposed by continuous processing of moving substrates, and those implemented to decrease costs and increase throughput. It is, therefore, beneficial to understand the tolerance of the established laboratory processes to variations in deposition procedures.

Research under this program consists of four basic parts to examine the tolerance of the established laboratory process to variations in deposition procedures:

1. Setting up the National Renewable Energy Laboratory (NREL)-developed three-stage CIGS laboratory process in a bell jar.

2. Characterizing the GSE roll-to-roll production chambers and device finishing steps in terms of the variables important to the laboratory processes.

3. Using the bell jar system to step incrementally from the NREL process to the conditions experienced by a sample during manufacturing, and characterizing the resulting films and devices.

4. Applying the process sensitivity information gained from the bell jar system to the production systems.

Some portions of these tasks are being performed in parallel. This quarter, activities related to maximum Cu ratio during CIGS growth, roll-coater temperature and flux profiles, post-CIGS processing, and bell jar processing were performed.

2. MAXIMUM CU RATIO DURING CIGS GROWTH

It was described last quarter that, for three-stage devices made in ITN's bell jar, maximum Cu ratio during CIGS growth has a large effect on device performance. This quarter, work to extend and examine these conclusions for GSE's production systems was performed. This work includes modifying the Ga profile of the bell jar devices to match the production devices, performing maximum Cu ratio tests in the production systems, and implementing initial thermopile monitoring of the production web.

2.a Ga profile

For devices in ITN's bell jar, a large effect of maximum Cu ratio during CIGS growth on device performance has been demonstrated. However, an exact translation of this process dependency to GSE's production roll-coaters is uncertain, as differences in Ga content and profile exist between the systems. Thus, attempts have been made to reproduce GSE's Ga profile in bell jar samples, allowing a repeat of maximum Cu ratio experiments in devices with a Ga profile similar to production devices.

Composition profiles of four bell jar devices were measured by Auger emission spectroscopy (AES) at the University of Illinois (UI) and compared with earlier UI AES data on GSE production devices. The AES data revealed that: 1) The GSE production and ITN bell jar devices exhibit a Ga profile similar enough that experiments regarding the effect of maximum Cu ratio can now be repeated using the new Ga profile, 2) bandgap does not seem to be culprit in variability (9.5% versus 12.5% efficiency) of baseline CIGS devices from the ITN bell jar, and 3) the current sample set, in conjunction with an awareness of the Ga deposition flux profiles, provides a good basis for extrapolating to new Ga profiles as needed.

A comparison of Ga depth profiles resulting from bell jar and roll-coater flux profiles is shown in Figure 1. Samples shown are typical GSE material (blue and pink), the previous bell jar baseline Ga profile (yellow), and a bell jar imitation of the roll-coater Ga profile (red). The production devices and the bell jar imitation exhibit very similar Ga profiles. The Ga notch is slightly less pronounced in the bell jar device, most possibly due to more diffusion as a consequence of lower deposition rates. The production and new bell jar devices are similar enough to repeat the maximum Cu ratio experiments with the new Ga profile.
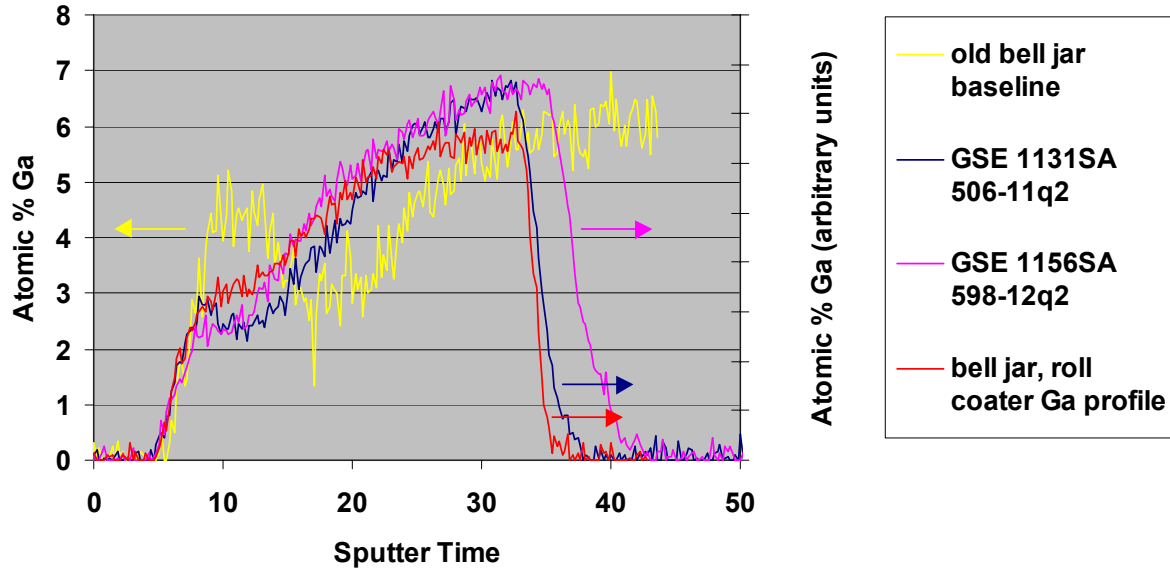
Figure 1: AES measurements from UI of atomic percent Ga profile, for two roll-coater samples (pink and blue), an bell jar imitation of the roll-coater Ga profile (red), and the previous bell jar baseline process (yellow).

Comparison of AES data from two bell jar samples provides an assessment of the reproducibility of ITN's bell jar Ga profile and its effect on efficiency. Figure 2 shows bandgap as a function of distance into the CIGS for these samples. The formula presented by Rockett[1] was used to convert Ga/(In+Ga) into bandgap. Samples B031009-1 (η=9.1%, V_{oc}=0.503V, J_{sc}=29.9mA/cm^2, ff=0.61) and B030826-1 (η=12.5%, V_{oc}=0.547V, J_{sc}=33.6mA/cm^2, ff=0.68) have similar bandgap profiles. The bandgap notch is slightly better defined for sample B030826-1, possibly because the average stage 2 and 3 temperature for B030826-1 was 510°C, not 575°C, implying slower Ga diffusion. To construct Figure 2, only the portion of the AES data considered to be from the CIGS was used. The front of the CIGS film was taken to be where atomic percent Cd decreased below 1 and depth profiles were truncated at the back of the CIGS where atomic Mo content reached 50%.
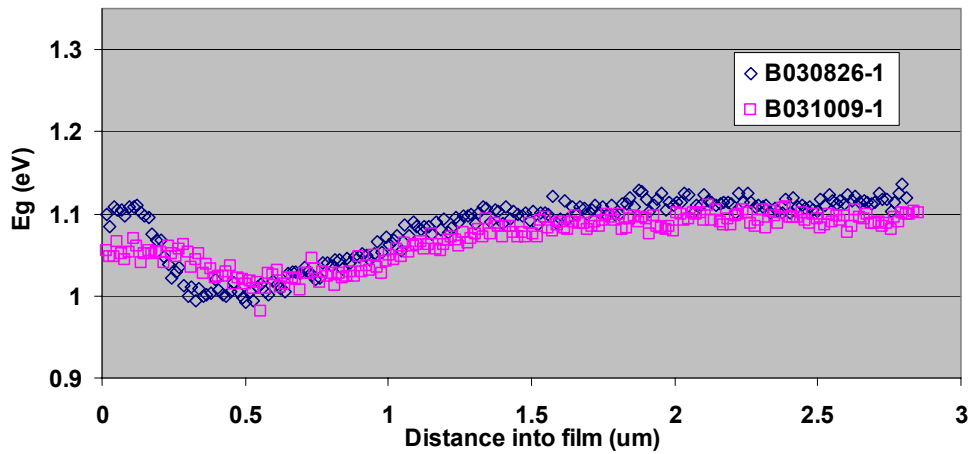

Figure 2: Bandgap as a function of distance into film for recent AES samples.

---

[1] A. Rockett, "Performance limitations in Cu(In,Ga)Se$_2$-based heterojunction solar cells", *Proceedings of the 29th IEEE Photovoltaic Specialists Conference*, pp. 587-591, (2002).

Modeling was then used to assess whether the minor band profile differences of Figure 2 might account for the performance differences between B031009-1 and B030826-1. ADEPT models were created setting most parameters as recommended by Gloeckler et al.[2] for CIGS. Bandgap was adjusted to match the profiles of Figure 2. Trap density was set 5× larger, as suggested by recent team admittance spectroscopy and drive-level capacitance comparisons of ITN and GSE CIGS with NREL CIGS. To assess the impact of slight bandgap differences, *only* modeled bandgap was changed in this comparison. Modeling predicts slightly favorable results from the B031009-1 bandgap profile, whereas B030826-1 measures higher in efficiency and voltage. Thus, modeling solely based on input variations in bandgap fails to predict the observed performance disparity between B030826-1 and B031009-1. It is, therefore, likely that materials properties **other** than bandgap – e.g., defect density (which in itself can be a consequence of changes in E_g) – are responsible for the performance differences in those devices.

As expected, Ga profiles measured by AES are related to the deposition flux profiles. Figure 3 shows two quantities for each bell jar sample. The blue line represents the AES Ga profile, in terms of atomic percent Ga, graphed from the back of the film to the front. Superimposed on the AES data, as a green line, is a smoothed profile of atomic percent Ga deposition flux as a function of time (or equivalently as a function of distance from the back of the film). Smoothing parameters were chosen empirically, but are identical for all samples, as overall deposition times and maximum deposition temperatures were similar. AES data are scaled along both axes to match XRF data. Figure 3 illustrates that the bandgap at the front of the film and the depth of the bandgap notch are clearly related to the amounts of Ga deposited in the first and third stages. A simple smoothing of deposition fluxes is only semi-qualitative, as a rigorous description of the physical phenomena occurring during film growth is not attempted. However, the current sample set, in conjunction with an awareness of the Ga deposition flux profiles, provides a good basis for extrapolating to new Ga profiles as needed.

Utilizing the new Ga profile, bell jar experiments quantifying the importance of the Cu-rich growth excursion are currently being repeated.

2.b Cu Ratio Tests in Production Systems

Tests of maximum Cu ratio during growth are also underway in the production systems. A two-level screening test of Cu-rich excursion and final Cu/(Ga+In) was performed in one of the CIGS production chambers (CIGS3) on lot 1472SA. The 2 × 2 matrix was replicated one time for a total of eight test conditions. The planned levels for Cu-rich excursion were 1.0 and 1.1, as measured by in-situ XRF. The planned levels for final composition (Cu/(Ga+In)) were 0.81 and 0.91. The web was processed according to baseline process conditions through production cell fabrication and measurement. Three sample panels were extracted from each condition, for a total of thirty sample cells for each. Deletion of outliers well outside the normal distribution was performed prior to analysis.

---

[2] M. Gloeckler, A.L. Fahrenbruch, J.R. Sites, "NUMERICAL MODELING OF CIGS AND CdTe SOLAR CELLS: SETTING THE BASELINE", *Proceedings of the Third World Conference on Photovoltaic Energy Conversion*, 2003.
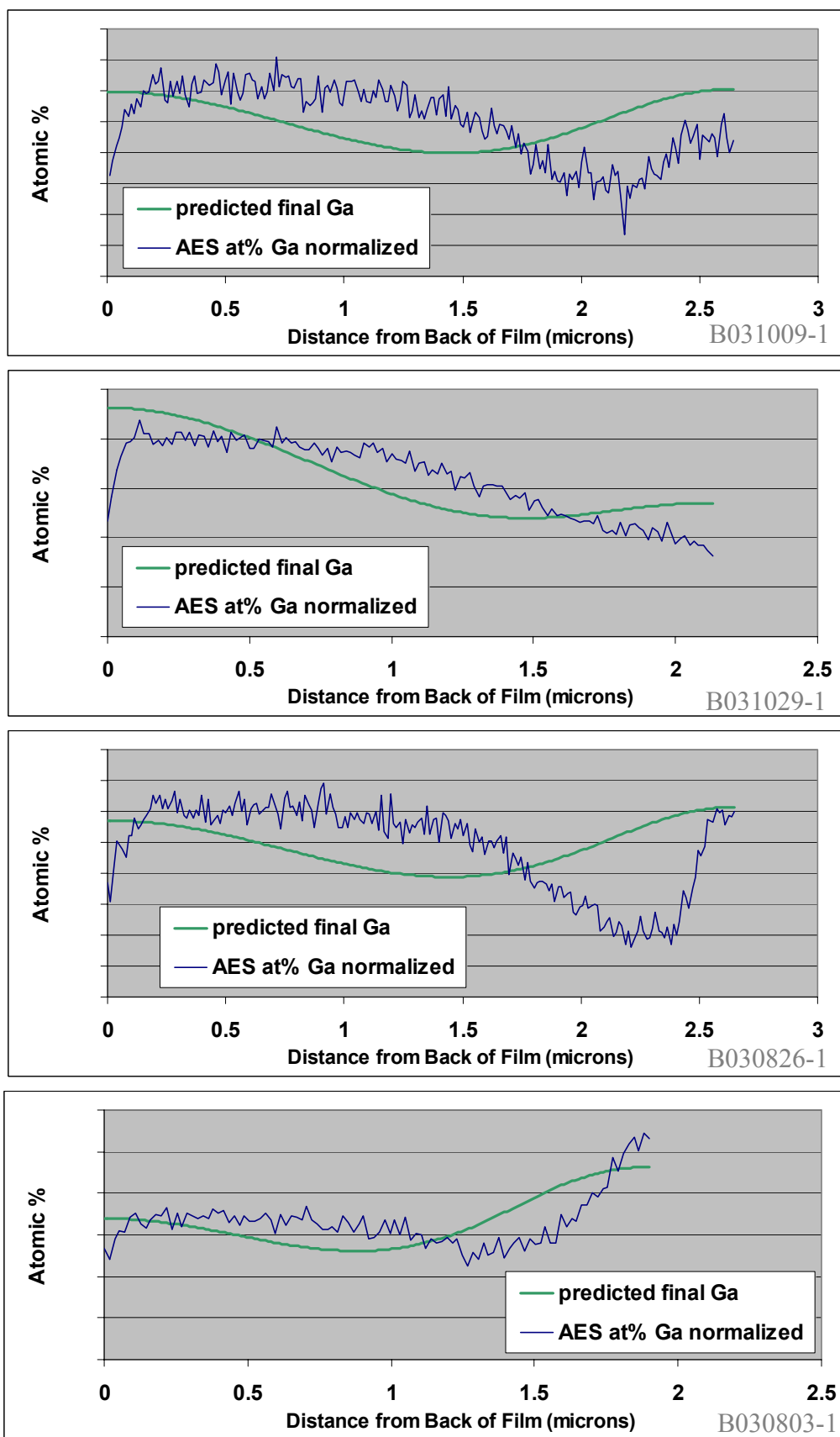
Figure 3: AES data with Ga profiles estimated from deposition fluxes.

The mean IV characteristics of each condition are plotted on the interaction charts in Figure 4. For films processed without a Cu-rich excursion (in process Cu/(Ga+In) ~ 1.0), the final composition had a significant effect on final efficiency; a final Cu/(Ga+In) of 0.91 was superior to 0.81. All IV parameters (V_{oc}, I_{sc}, and fill factor) improved. For films that experienced a Cu-rich excursion (in process Cu/(Ga+In) ~ 1.1), the efficiency was much less dependent on the final Cu/(Ga+In). The latter process was more robust, although the mean efficiency under the best conditions may be slightly lower than the case where the film did not go Cu-rich.
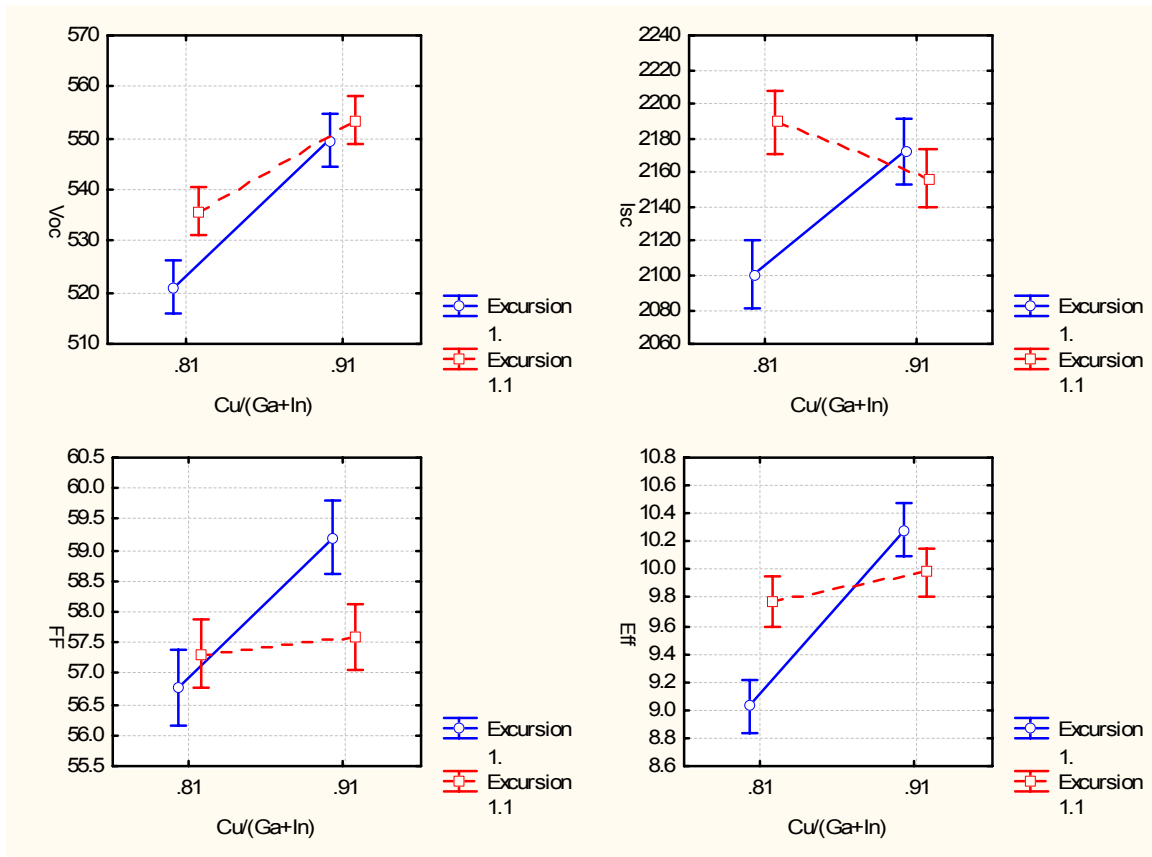

Figure 4: Interaction charts summarizing device parameters from roll-coaters as a function of maximum and final Cu ratio.

2.c Monitoring in Production Systems

Efforts to apply sensing of the Cu-rich growth excursion in the production systems, similar to what has been implemented in the bell jar, are also underway. The use of a thermopile to monitor the Cu-rich growth excursion in the bell jar was described in previous quarterly reports. This quarter, the thermopile was modified to withstand higher temperatures and installed in the CIGS4 production roll-coater. An example of thermopile signal as a function of web position is shown in Figure 5. After one month of operation in the production chambers, the thermopile is no longer responsive. It is currently unclear whether the features in the thermopile signal are due to CIGS properties or intermittant sensor malfunction. When processing of web G40396 is complete, device parameters as a function of web position will be compared with the IR signal.
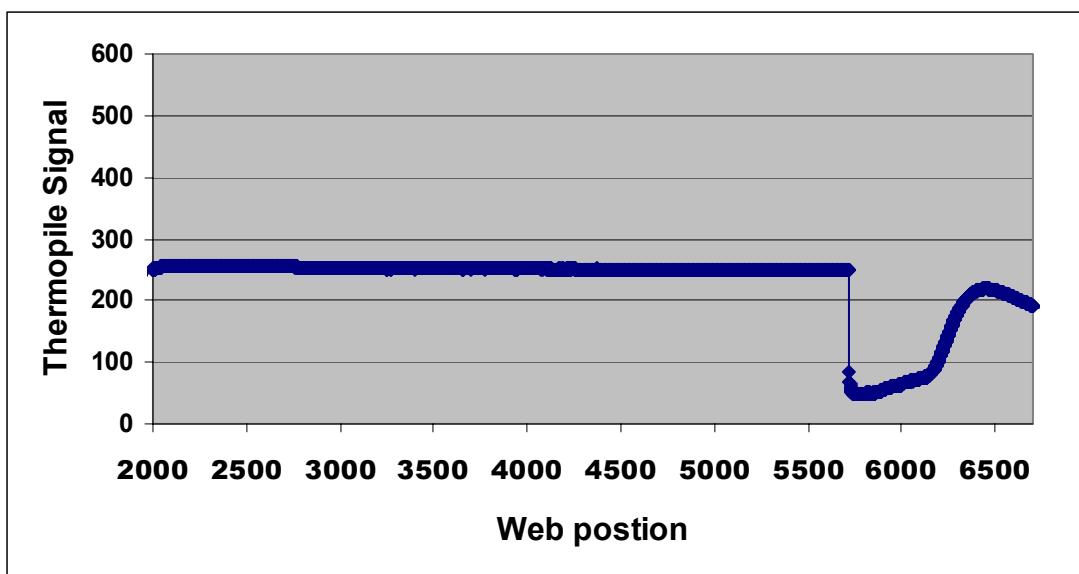
Figure 5: Thermopile signal versus web position for production deposition G40396.

3. ROLL-COATER TEMPERATURE AND SOURCE FLUX PROFILES

Bell jar processing is being used to assess the impact of temperature and flux profiles encountered in the production systems.

Standard three-stage laboratory CIGS deposition entails two temperatures: a low ($\sim$350^{o}C) temperature during the initial group III fluxes, and a high ($\sim$ 575°C) temperature during the remaining two stages.[3] The temperature experienced by the growing CIGS film in a production system may differ due to source placement, movement of the substrate between zones, and substrate thermal mass. The impact of differences between the laboratory and production temperature profiles was assessed this quarter.

CIGS depositions were performed on 3" $\times$ 3" glass substrates in the bell jar. Some depositions were performed using a standard 350°C/575°C laboratory temperature profile. Other depositions were performed using an approximation of the production system temperature profile. The approximate roll-coater temperature profile was obtained in earlier experiments at GSE, using thermocouples attached to the moving web. Conditions other than temperature profile, such as deposition times and rates, were held constant.

Device efficiency for the different temperature profiles are shown in Figure 6. Purple triangles show individual device efficiencies from each of 51 devices on 6 substrates. Devices are 1 cm^2, measured under AM1.5 total-area conditions, without anti-reflective (AR) coating. Dark blue data points are are the average efficiency for each condition, with error bars showing $\pm$ one standard deviation. No impact on device performance is apparent from the differences in temperature profile.

---

[3] A.M. Gabor, J.R. Tuttle, D.S. Albin, M.A. Contreras, R. Noufi, A.M. Herman, "High-efficiency CuIn$_x$Ga$_{1-x}$Se$_2$ solar cells made from (In$_x$,Ga$_{1-x}$)$_2$Se$_3$ precursor films", *Applied Physics Letters*, **65**(2), (1994), pp. 198-200.
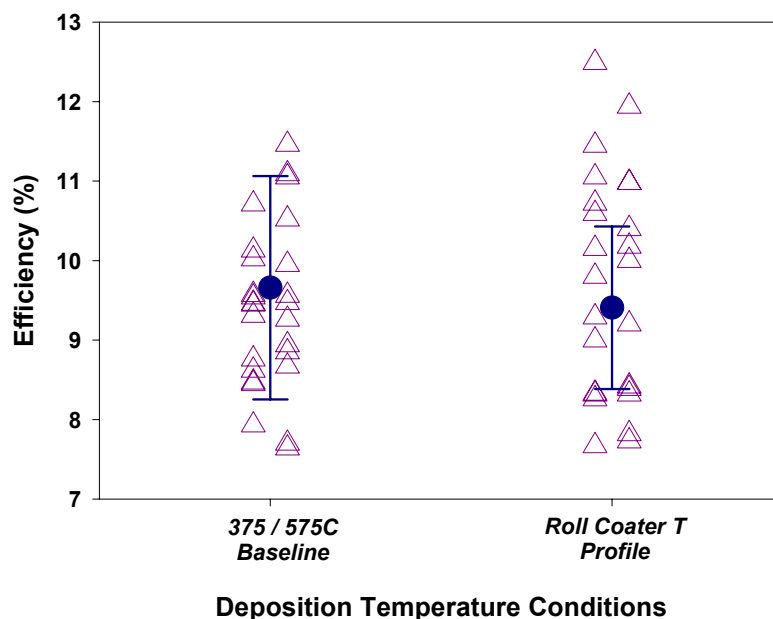
Figure 6: Comparison of device efficiencies from bell jar utilizing standard 350°C/575°C temperature profile or one similar to what is encountered in production system.

Metals flux profiles are another aspect of CIGS deposition that differs between the laboratory and production systems. Characterization of metals fluxes as a function of position was described in earlier reports. The implications for three-stage CIGS deposition are reviewed in Figure 7, where Figure 7a shows the flux as a function of position (or equivalently time, for the moving production substrate) from a roll-coater Cu source. Figure 7b illustrates the standard laboratory three-stage flux profiles, and Figure 7c depicts the bell jar three-stage flux profiles modified to deposit a film of similar composition and thickness, while imitating the flux vs. time seen by a substrate in the roll-coater. The flux profiles of Figure 7c were created by varying with time the setpoint assigned to the electron impact emission spectrometer rate controller. The insets in Figure 7b and Figure 7c show efficiencies for devices made using each type of flux profile. These preliminary results may indicate a detrimental effect on efficiency from the peaked metals flux profiles. Currently depositions are being performed using the peaked metals flux profiles in combination with a variety of Se rates, to determine if the harmful effect is a function of instantaneous Se-to-metals ratio. The repeated experiments will also minimize the effect of run-to-run bell jar variability (as evident in the error bars of Figure 6) on conclusions.

4. POST-CIGS PROCESSING

Study of sensitivities of several processing steps subsequent to CIGS deposition is also underway.

4a. Venting

The effect of CIGS chamber venting temperature was examined as to its potential impact on device efficiency. Although typical laboratory procedures call for cooling CIGS substrates to near room temperature before venting the CIGS chamber, higher venting temperatures are desirable for maximizing throughput. To investigate this issue, nominally identical CIGS

The table in panel b):

CIGS deposition	η (%)	Voc (V)	Jsc (mA/cm²)	Ff
B031008-2	8.0	0.473	33.1	0.51
B031029-2	9.9	0.541	29.6	0.62

The table in panel c):

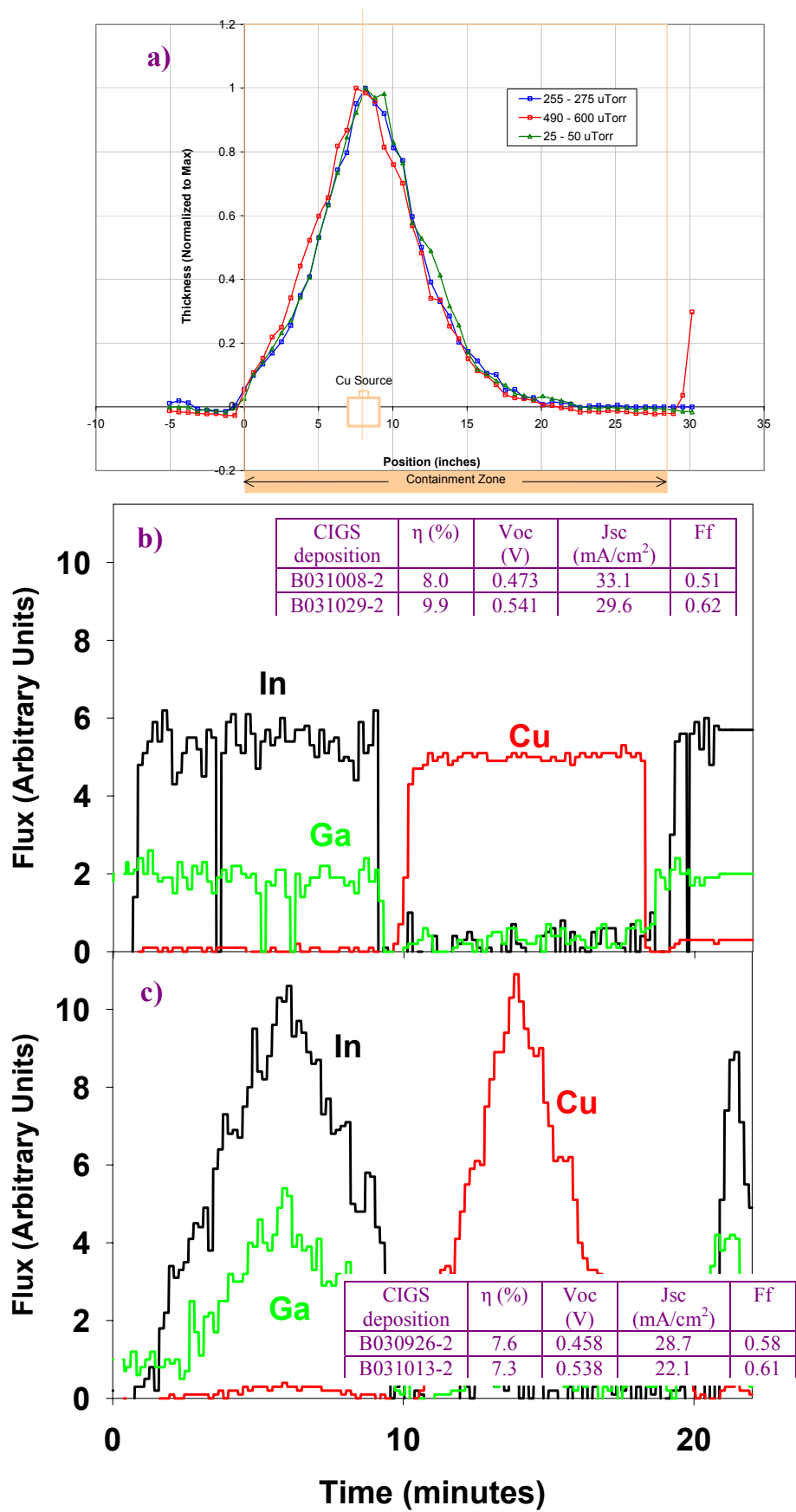| CIGS deposition	η (%)	Voc (V)	Jsc (mA/cm²)	Ff
B030926-2	7.6	0.458	28.7	0.58
B031013-2	7.3	0.538	22.1	0.61

Figure 7: Flux profile a) measured in roll-coater, b) used in bell jar for standard three stage recipe, and c) used in bell jar to imitate roll-coater.

depositions were performed on 3" × 3" glass substrates in the bell jar. After deposition, the substrate was allowed to cool in vacuum for varying amounts of time. Device efficiency as a function of venting temperature is shown in Figure 8. Green circles show individual device efficiencies from each of 89 devices on 10 substrates. Dark blue data points are the average efficiency for each condition, with error bars showing ± one standard deviation. For the highest venting temperature (300°C), a slightly different procedure was followed to prevent significant formation of H_2Se. At 300°C, the hi-vac valve was closed to stop pumping and allow gradual leak-up of chamber pressure, but chamber was not fully vented until cool. In each case, there is no measureable impact of the venting temperature on device performance.
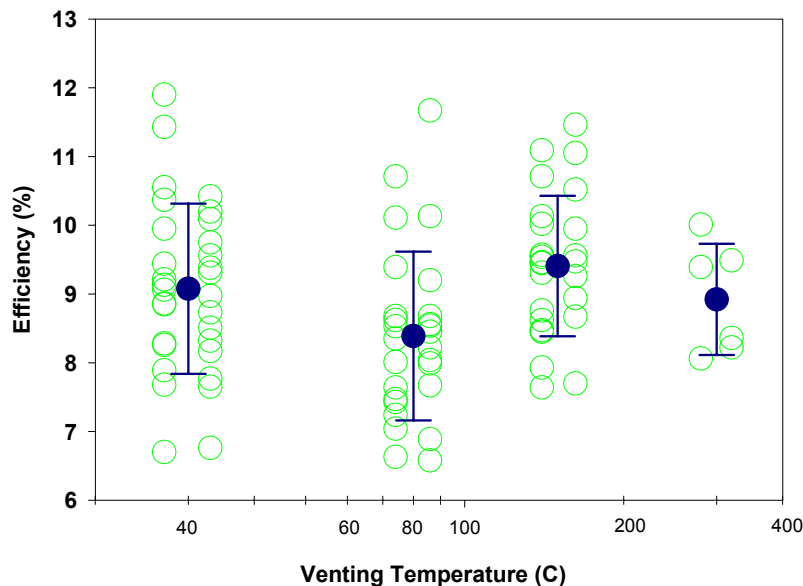

Figure 8: Device efficiency as a function of venting temperature.

4b. Cool-down

The effect of post-deposition CIGS cool-down conditions was also examined for impact on device efficiency. CIGS was deposited on 3" × 3" substrates utilizing the same conditions up to the end of the third stage. After the end of the third stage, samples were allowed to cool at different rates. Under the first cool-down condition, the samples spent 200 seconds above 400°C, the maximum cooling rate of glass in the bell jar. Under the second cool-down condition, the samples spent 250 seconds above 400°C, a cooling rate based on the motion of the web through a roll-coater. Se flux was either turned off immediately at the end of stage 3, or delivered at the stage 3 rate until the substrate temperature dropped below 400°C. Results are shown in Figure 9. Red circles show individual device efficiencies from each of 115 devices on 10 substrates. Dark blue data points are the average efficiency for each condition, with error bars showing ± one standard deviation. Conditions in Figure 9 correspond to those typically utilized in the laboratory and in production. Over the range explored, there is no measureable impact of the cool-down conditions on device performance.
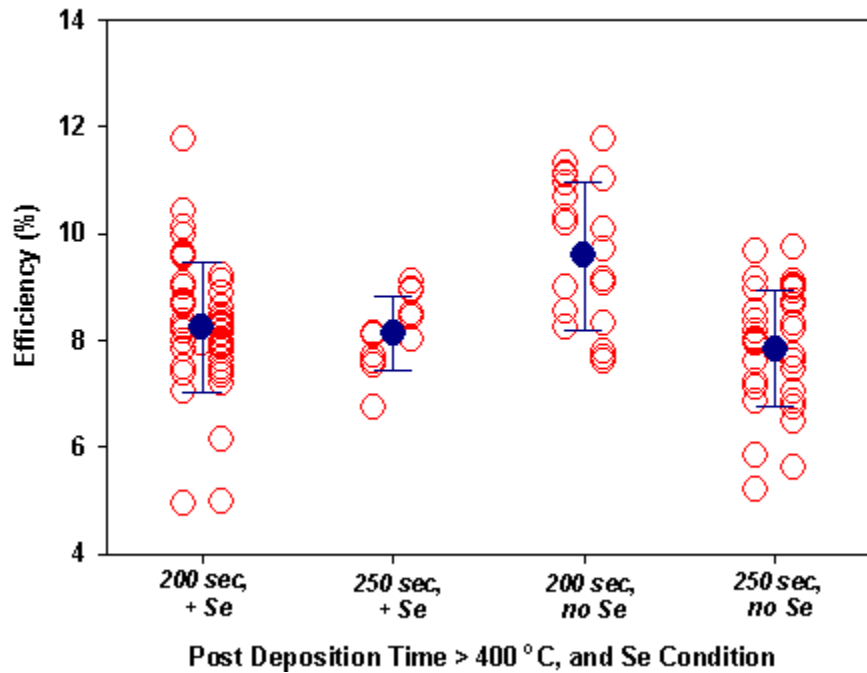
Figure 9: Device efficiency as a function of post-CIGS deposition cool-down conditions.

4c. Surface Treatment

CIGS surface passivation and improved junction formation is being investigated via thioacetamide treatment.[4,5]   Design of experiments is being used to optimize treatment temperature, time, concentrations, and salt for the GSE production material. Results will be reported when analysis of the first experimental matrices is complete.
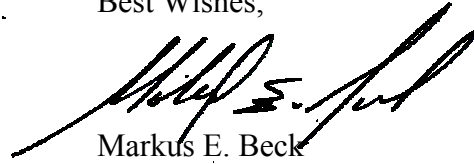

5. BELL JAR PROCESSING

In parallel with the activities described above, several examinations are underway to increase the performance of the best devices from the ITN bell jar, and decrease their variability. The purpose of these improvements is threefold: 1) process sensitivies are best explored in a higher performance envelope to keep pace with rising product performance; 2) identifiable factors that increase performance and decrease variability in the bell jar can also likely be applied to roll-coater processing; and 3) a decrease in variability allows drawing strong conclusions while performing fewer experiments. A 12-14% efficiency envelope has been identified a goal for baseline bell jar devices. (Quoted efficiency is total-area, without AR coating.) Toward this goal, the examinations being performed are quantifying the role of the substrate or Na in variability, quantitative comparison of NREL and ITN device finishing, finer control of film thickness and maximum Cu ratio, comparison of very high efficiency NREL processing conditions with those currently applied at ITN, and inspection of scanning electron

---

[4] T. Wada, Y. Hashimoto, S. Nishiwaki, T. Satoh, S. Hayashi, T. Negami, H. Miyake, "High efficiency CIGS solar cells with modified CIGS surface," *Sol. En. Mtls. & Sol. Cells*, **67**, (2001), pp. 305-310.
[5] T. Nakada, K. Matsumoto, M. Okumura, "Improved Efficiency of Cu(In,Ga)Se$_2$ Thin Film Solar Cells by Surface Sulfurization Using Wet Process," *Proc. of the 29th IEEE PVSC*, (2002).

micrograph and x-ray diffraction data from devices of varying efficiency to suggest processing changes.

Best Wishes,

Markus E. Beck

Cc: Carolyn Lopez, NREL Subcontract Associate